ELSEVIER

Microporous and Mesoporous Materials 41 (2000) 107–118

MICROPOROUS AND MESOPOROUS MATERIALS

www.elsevier.nl/locate/micromeso

Dehydration mechanism in brewsterite: single-crystal X-ray diffraction study

Michele Sacerdoti [a], Giovanna Vezzalini [b,*], Simona Quartieri [c]

[a] *Istituto di Mineralogia, C.so Ercole I° d'Este 32, I-44100 Ferrara, Italy*
[b] *Dipartimento di Scienze della Terra, via S. Eufemia 19, I-41100 Modena, Italy*
[c] *Dipartimento di Scienze della Terra, Salita Sperone 31, I-98166 Messina – S. Agata, Italy*

Received 17 April 2000; received in revised form 14 July 2000; accepted 20 July 2000

Abstract

The crystal structure of the zeolite brewsterite (space group $P2_1/m$, ideal formula $(Sr,Ba)_2Al_4Si_{12}O_{32} \cdot 10H_2O$) was studied at different dehydration levels. Six single crystals were kept in evacuated capillaries at different temperatures and for different treatment times, and the X-ray diffraction data were collected at room temperature. The following results were obtained.

1. The structure refinements of the partially dehydrated brewsterite indicate that, as dehydration advances, the cell volume decreases, the channels are contracted and the exchangeable cations spread over several sites, which were occupied in the original structure by water molecules. These results are in agreement with a previous in situ powder diffraction study.

2. The T–O–T bridge breaking and the consequent formation of new 4- and 5-coordinated (Si,Al) polyhedra, already observed in a previous single-crystal dehydration study, are caused by the necessity of the exchangeable cations to be coordinated by the framework oxygens when the water loss is almost complete. This phenomenon was not observed in the in situ powder diffraction experiment, probably owing to the presence of residual water.

3. The effect of the heating time was also evaluated: a longer exposure of the crystal at high temperature in vacuum favors a higher percentage of T–O–T bridge breaking, and induces the complete depopulation of the original Sr site, with a wider spreading of the extra-framework cations.

Keywords: Brewsterite; Dehydration; Single-crystal XRD; Phase transformation; T–O–T bridge breaking

1. Introduction

Brewsterite is a zeolite of the heulandite group characterized by the 4^25^4 unit, with the space group $P2_1/m$ and the ideal formula $(Sr,Ba)_2Al_4Si_{12}O_{32} \cdot 10H_2O$. In the framework of brewsterite, these units share a branch with two adjacent units, generating a chain parallel to the *a* axis. The chains are connected by single 4-rings to form sheets parallel to (0 1 0); the sheets are bridged by oxygen atoms lying on (0 1 0) mirror planes [1,2] (Fig. 1).

Investigations on the dehydration behavior of zeolites are usually performed following two different and complementary approaches:

* Corresponding author. Tel.: +39-059-2055827; fax: +39-059-2055887.
E-mail address: giovanna@unimo.it (G. Vezzalini).

1387-1811/00/$ - see front matter
PII: S1387-1811(00)00278-X

- X-ray diffraction at room temperature on single crystals, previously dehydrated in vacuum at selected temperatures and subsequently sealed in glass capillaries. This technique gives very detailed information on the structure of the phases at different dehydration steps, but not on the dynamics and kinetics of the process;
- in situ synchrotron X-ray powder diffraction. This technique, based on full-profile Rietveld structural analysis, provides specific information on the dynamics of the temperature-induced transformations.

These methodologies are based on experimental conditions (use of vacuum or inert gas flow, heating rate, heating time, crystal dimensions, etc.) which can be very different, so the results are not usually comparable. To reach a complete understanding of the dehydration mechanism in zeolites, it is therefore important to perform detailed investigations using both techniques.

In a previous paper, the dehydration behavior of a sample of brewsterite from Strontian (Scotland) was studied by heating two crystals at 280°C and 330°C (BR280 and BR330, respectively) for 24 h under high vacuum in a quartz capillary; X-ray data collection was carried out at room temperature [3]. The main consequences of the almost complete dehydration were a marked decrease of the unit cell, and the statistical breaking of one T–O–T bridge of the 4-ring (T1–O7–T2). [1] As a consequence of T–O–T breaking, in BR280, the T1 cation migrated (in 31% of cases) to a new tetrahedral site (labeled T11 with a site occupancy of 0.31), sharing three vertices with the one previously occupied. The fourth vertex (O71) is on the mirror plane, and joins (in nearly 50% of cases) two adjacent tetrahedral layers. In the remaining 50%, it is unshared and bound to a hydrogen atom to form an OH^- group, as shown by Alberti et al. [9] by means of μ-IR spectroscopy. The T2 cation migrates (in 20% of cases) to a fivefold coordinated site (labeled T21 with a site occupancy of 0.20), sharing three vertices with the previously occupied tetrahedron. The fourth vertex (O72) is on the mirror plane and joins (in about 33% of cases) two adjacent layers, while the fifth vertex (O73), presumably an OH^- group, is unshared. The new T–O–T bridges prevent the immediate rehydration of the heated brewsterite. Moreover, the exchangeable cations, which occupy only one extra-framework site in the untreated brewsterite, spread over several sites.

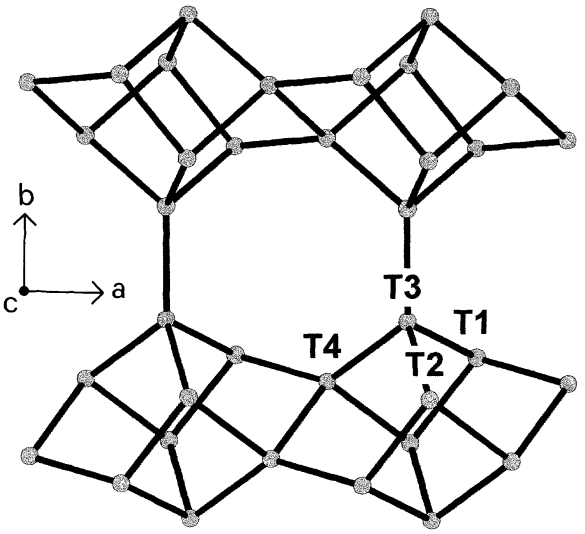

Fig. 1. Structure of brewsterite viewed along the *c* axis.

Ståhl and Hanson [10] studied the dehydration process of brewsterite by in situ X-ray synchrotron radiation powder diffraction. They demonstrated that, as water is being expelled, three alternative cation sites appear in succession. These have more framework oxygens in their coordination spheres and/or show an increasing ability to share water molecules with each other. This study did not extend to a complete dehydration of brewsterite, and did not indicate any T–O–T bridge breaking.

In this paper, we follow the dehydration process of brewsterite, working on several single crystals kept under vacuum at different temperatures and for different heating times.

The aims of this work are

1. to describe the effect of different degrees of dehydration on the brewsterite framework and on the distribution of the extra-framework species;

[1] This unusual framework modification was also observed in all the other zeolites characterized by the $4^2 5^4$ unit [4–8].

2. to verify under which dehydration conditions T–O–T breaking and the formation of new 4- and 5-coordinated T polyhedra are observed;
3. to understand the effect of different treatment times on the extent of T–O–T breaking and (Sr,Ba) spreading at the same temperature (330°C).

2. Experimental and structure refinement

The brewsterite crystals used in this work are from Strontian (Scotland). Electron microprobe analysis performed on many crystals of this brewsterite showed a strong variability in the Sr/Ba ratio, whereas no variability was observed in the Si/Al ratio (Table 1, footnote). Due to the impossibility of analyzing the crystals used for the dehydration experiments, the chemical formula given by Schlenker et al. [1] is assumed in this work (Table 1, footnote). Dehydration experiments were performed by inserting the crystals in a quartz capillary (with walls approximately 0.025 mm thick) evacuated at 10^{-6} bar, heated at different temperatures and for different times (Table 1), then sealed and cooled to room temperature. Next, X-ray data were collected at room temperature; the heating conditions and instrumental parameters of these data collections are reported in Table 1. The BR330s sample is the same crystal as that labeled BR330 in Ref. [3]. The X-ray diffraction data were collected in a whole hemisphere for all samples (MoKα radiation, graphite monochromator), then corrected for Lorentz and polarization effects and for absorption using different methods (Table 1). Atomic scattering factors for neutral atoms were used with real and imaginary dispersion correction; the Sr scattering curve was used for extra-framework cation sites, and the oxygen curve for the water molecule ones. Cell parameters and other refinement data are reported in Table 1 along with crystallographic data for the untreated brewsterite (BRNAT, [1]). Refinements were performed using the SHELXL computer program [11] in the space group $P2_1/m$, starting from the framework atom coordinates of Schlenker et al. [1]. Coordinates of Sr and water molecule sites were obtained by difference Fourier synthesis. Peaks with a height less than 1 or 2 $e^-/Å^3$ but with a distance less than 1 Å from Sr sites, here considered as ripples, were not refined. Owing to the severe crystal fracture, only 600 unique reflections were used in the refinement of the BR330s sample, and so the results of the structural refinement are rather poor.

In the following discussion, the original Sr site, present in the untreated brewsterite, is labeled Sr as in Schlenker et al. [1], while for the other Sr sites, the nomenclature adopted by Alberti et al. [3] is used.

Coordinates, thermal factors and occupancies of all atoms are reported in Table 2, selected bond distances and angles for the tetrahedral atoms in Table 3, and the Sr polyhedra in Table 4.

3. Results

As observed in previous dehydration studies [12–14], zeolites can also lose water molecules at room temperature by maintaining the samples under high vacuum or in inert gas flow for a long time, and thus avoiding the possible fracture of the crystals induced by high temperature. For this reason, we performed some dehydration tests at room temperature for different treatment times: 24 (BR24h) and 96 h (BR96h), respectively.

In BR24h, the weak water loss was restricted to W1 and W2 sites and induced a unit cell contraction of about 1%. A larger decrease in the cell volume was observed in BR96h (1.5%), where a larger water loss occurred in the same sites. In both samples, negligible framework modifications were observed, and the extra-framework cations were still only in the Sr original site. The high occupancy factor of the Sr site (Table 2) can be justified by the higher Ba content of our two crystals with respect to Schlenker's sample [1].

Besides the room temperature tests, we performed dehydration tests at different temperatures (100°C, 180°C and 330°C). In BR100, the unit cell volume was about 3% less than that of untreated brewsterite. At this temperature, the spreading of the extra-framework cations began. In fact, the occupancy of the Sr site decreased, while the number of electrons at the W3 site (labeled Sr1

Table 1
Experimental and crystallographic data for brewsterite samples[a]

	BRNAT	BR24h	BR96h	BR100[b]	BR180[b]	BR330f[c]	BR330s[b]
T (°)	–	rT	rT	100	180	330	330
Treatment time (h)	–	24	96	24	80	0.5	24
a (Å)	6.793(2)	6.776(3)	6.780(1)	6.804(1)	6.785(1)	6.785(1)	6.627(3)
b (Å)	17.573(6)	17.466(3)	17.455(2)	17.285(3)	16.988(3)	16.988(1)	16.400(6)
c (Å)	7.759(2)	7.722(1)	7.705(1)	7.645(1)	7.645(1)	7.657(1)	7.484(1)
β (°)	94.54(3)	94.47(2)	94.59(1)	94.60(1)	94.60(1)	94.64(1)	94.04(2)
V (Å^3)	923.3	911.1	908.9	896.2	878.3	879.7	811.4
ΔV (%)	–	−1.3	−1.5	−2.9	−4.9	−4.7	−12.1
Instrument		CAD4 Nonius	CAD4 Nonius	Siemens PR4A	Siemens PR4A	KCCD Nonius	CAD4 Nonius
Max 2θ (°)		60	60	57	50	60	52
Unique reflections		2733	2724	2348	1506	2630	1614
R_{eq} (%)		3.5	4.3	4.1	9.2	6.3	4.6
Reflection used in the refinement		2009	2125	2011	918	1974	600
Final R_w (%)		3.46	4.24	6.41	8.64	7.55	8.40
Crystal dimensions (mm^3)		0.36 × 0.19 × 0.07	0.20 × 0.14 × 0.05	0.20 × 0.16 × 0.06	0.10 × 0.10 × 0.02	0.26 × 0.10 × 0.04	0.46 × 0.21 × 0.16
Absorption correction method		[16]	[16]	[16]	[16]	[17]	[18]
Extra-framework cation electrons	81	85	92	98	82	86	71
Water molecules	10	9.56	8.73	3.12	2.12	0.79	0.0

[a] Chemical formula: $K_{0.02}Ba_{0.48}Sr_{1.42}Al_{4.12}Si_{11.95}O_{32} \cdot 10H_2O$ [1]. Variability ranges for Sr and Ba as determined by electron microprobe analysis on several different crystals of brewsterite from Strontian: Ba 0.41–1.22 and Sr 0.86–1.57.

[b] Heating rate: 1.5°C/min.

[c] Heating rate: 10°C/min.

Table 2
Atomic coordinates, occupancy (%) and temperature factors (U_{eq} or U_{iso}, Å^2) for brewsterite samples[a]

		BRNAT	BR24h	BR96h	BR100	BR180	BR330f	BR330s
T1	*x*	0.3218(2)	0.3225(1)	0.3237(1)	0.3289(2)	0.3240(5)	0.3228(2)	0.323(2)
	y	0.0812(1)	0.0821(1)	0.0825(1)	0.0865(1)	0.0869(2)	0.0860(1)	0.089(1)
	z	0.8224(2)	0.8225(1)	0.8232(1)	0.8241(2)	0.8221(4)	0.8204(2)	0.830(2)
	U_{eq}	0.0139	0.0117(2)	0.0101(2)	0.0126(3)	0.0244(9)	0.0315(4)	0.096(5)
	occ	1.0	1.0	1.0	1.0	1.0	0.935(5)	0.600(11)
T11	*x*						0.2515(40)	0.230(3)
	y						0.1579(18)	0.161(1)
	z						0.8409(36)	0.854(3)
	U						0.0503(58)	0.096(5)
	occ						0.065(5)	0.400(11)
T2	*x*	0.4054(2)	0.4040(1)	0.4032(1)	0.3974(2)	0.4012(5)	0.4030(2)	0.405(2)
	y	0.0566(1)	0.0564(1)	0.0556(1)	0.0539(1)	0.0598(3)	0.0611(1)	0.068(1)
	z	0.2108(2)	0.2104(1)	0.2115(1)	0.2133(2)	0.2075(5)	0.2065(2)	0.189(2)
	U_{eq}	0.0151	0.0134(2)	0.0119(2)	0.0147(4)	0.0306(11)	0.0370(4)	0.115(4)
	occ	1.0	1.0	1.0	1.0	1.0	0.916(9)	0.756(10)
T21	*x*						0.2371(64)	0.228(6)
	y						0.3790(29)	0.133(2)
	z						0.2239(58)	0.192(5)
	U						0.1000(108)	0.115(4)
	occ						0.084(9)	0.244(10)
T3	*x*	0.5553(2)	0.5558(1)	0.5562(1)	0.5581(2)	0.5607(5)	0.5612(2)	0.569(1)
	y	0.1582(1)	0.1581(1)	0.1582(1)	0.1585(1)	0.1587(2)	0.1587(1)	0.161(1)
	z	0.5336(2)	0.5334(1)	0.5340(1)	0.5350(2)	0.5359(4)	0.5360(2)	0.535(1)
	U_{eq}	0.0138	0.0112(2)	0.0097(2)	0.0125(3)	0.0236(9)	0.0335(4)	0.104(5)
	occ	1.0	1.0	1.0	1.0	1.0	1.0	1.0
T4	*x*	0.9087(2)	0.9100(1)	0.9108(1)	0.9163(2)	0.9132(4)	0.9124(2)	0.907(2)
	y	0.0528(1)	0.0532(1)	0.0536(1)	0.0544(1)	0.0482(2)	0.0466(1)	0.043(1)
	z	0.6410(2)	0.6413(1)	0.6415(1)	0.6444(2)	0.6498(5)	0.6519(2)	0.659(1)
	U_{eq}	0.0128	0.0113(2)	0.0096(2)	0.0128(4)	0.0253(9)	0.0370(4)	0.104(5)
	occ	1.0	1.0	1.0	1.0	1.0	1.0	1.0
O1	*x*	0.3501(6)	0.3507(4)	0.3511(4)	0.3552(6)	0.3595(12)	0.3618(7)	0.343(4)
	y	0.1059(2)	0.1065(2)	0.1062(2)	0.1098(3)	0.1155(6)	0.1167(3)	0.112(2)
	z	0.0283(4)	0.0291(3)	0.0307(4)	0.0347(5)	0.0279(11)	0.0234(5)	0.010(3)
	U_{eq}	0.0225	0.0202(5)	0.0188(6)	0.0236(9)	0.0374(26)	0.0503(10)	0.273(20)
	occ	1.0	1.0	1.0	1.0	1.0	1.0	1.0
O2	*x*	0.4218(6)	0.4209(4)	0.4207(5)	0.4168(7)	0.4303(17)	0.4437(10)	0.486(3)
	y	0.1240(2)	0.1233(2)	0.1213(2)	0.1173(3)	0.1256(10)	0.1306(5)	0.134(1)
	z	0.3607(5)	0.3631(3)	0.3651(4)	0.3753(6)	0.3606(14)	0.3534(8)	0.332(1)
	U_{eq}	0.0294	0.0269(6)	0.0246(7)	0.0297(10)	0.0830(50)	0.1038(29)	0.189(14)
	occ	1.0	1.0	1.0	1.0	1.0	1.0	1.0
O3	*x*	0.7825(6)	0.7818(4)	0.7845(5)	0.7841(7)	0.7749(15)	0.7739(8)	0.784(3)
	y	0.1211(2)	0.1209(2)	0.1215(2)	0.1215(3)	0.1138(8)	0.1134(4)	0.117(1)
	z	0.5454(5)	0.5448(3)	0.5458(4)	0.5486(6)	0.5649(14)	0.5628(8)	0.590(3)
	U_{eq}	0.0244	0.0231(5)	0.0218(6)	0.0292(10)	0.0573(32)	0.0796(17)	0.167(12)
	occ	1.0	1.0	1.0	1.0	1.0	1.0	1.0
O4	*x*	0.4500(6)	0.4523(4)	0.4550(5)	0.4608(6)	0.4353(15)	0.4298(8)	0.430(4)
	y	0.1408(2)	0.1422(2)	0.1434(2)	0.1498(2)	0.1512(7)	0.1497(3)	0.149(1)

(*continued on next page*)

Table 2 (*continued*)

		BRNAT	BR24h	BR96h	BR100	BR180	BR330f	BR330s
	z	0.7150(5)	0.7163(3)	0.7190(4)	0.7253(5)	0.7075(13)	0.7041(7)	0.694(3)
	U_{eq}	0.0251	0.0234(5)	0.0216(6)	0.0224(8)	0.0498(30)	0.0693(15)	0.212(16)
	occ	1.0	1.0	1.0	1.0	1.0	1.0	1.0
O5	x	0.0850(6)	0.0872(4)	0.0880(4)	0.0953(6)	0.0872(12)	0.0848(6)	0.076(4)
	y	0.0920(2)	0.0927(2)	0.0933(2)	0.0972(3)	0.0911(8)	0.0910(4)	0.084(1)
	z	0.7615(5)	0.7600(4)	0.7591(4)	0.7583(6)	0.7688(13)	0.7674(7)	0.778(4)
	U_{eq}	0.0295	0.0259(6)	0.0240(7)	0.0293(10)	0.0535(33)	0.0695(15)	0.243(17)
	occ	1.0	1.0	1.0	1.0	1.0	1.0	1.0
O6	x	0.2228(6)	0.2203(5)	0.2203(5)	0.2096(7)	0.2021(16)	0.2060(9)	0.208(3)
	y	0.9966(2)	0.9963(2)	0.9954(2)	0.9959(3)	1.0062(9)	1.0097(5)	1.026(1)
	z	0.2388(6)	0.2369(4)	0.2352(5)	0.2264(7)	0.2249(16)	0.2275(10)	0.240(3)
	U_{eq}	0.0350	0.0341(7)	0.0296(8)	0.0309(10)	0.0737(44)	0.1067(29)	0.175(15)
	occ	1.0	1.0	1.0	1.0	1.0	1.0	1.0
O7	x	0.3851(6)	0.3888(4)	0.3906(4)	0.3987(7)	0.4044(13)	0.4040(7)	0.402(3)
	y	0.9921(2)	0.9930(2)	0.9936(2)	0.9977(3)	0.9981(6)	0.9971(3)	1.002(2)
	z	0.7952(5)	0.7961(3)	0.7957(4)	0.7945(6)	0.7990(12)	0.7971(6)	0.809(3)
	U_{eq}	0.0231	0.0216(5)	0.0185(6)	0.0252(9)	0.0370(25)	0.0542(11)	0.125(12)
	occ	1.0	1.0	1.0	1.0	1.0	1.0	0.699(17)
O71	x							0.100(4)
	y							0.25
	z							0.769(4)
	U							0.174(12)
	occ							1.0
O72	x							0.201(7)
	y							0.25
	z							0.198(7)
	U							0.134(23)
	occ							0.554(26)
O73	x							0.000(11)
	y							0.196(4)
	z							0.292(11)
	U							0.134
	occ							0.244(10)
O8	x	0.0	0.0	0.0	0.0	0.0	0.0	0.0
	y	0.0	0.0	0.0	0.0	0.0	0.0	0.0
	z	0.5	0.5	0.5	0.5	0.5	0.5	0.5
	U_{eq}	0.0403	0.0378(11)	0.0341(13)	0.0417(19)	0.0870(75)	0.1074(42)	0.144(19)
	occ	1.0	1.0	1.0	1.0	1.0	1.0	1.0
O9	x	0.5718(10)	0.5713(7)	0.5667(9)	0.5678(11)	0.5928(35)	0.6152(20)	0.635(4)
	y	0.25	0.25	0.25	0.25	0.25	0.25	0.25
	z	0.4994(8)	0.4948(6)	0.4905(7)	0.4728(9)	0.4902(29)	0.5069(17)	0.504(4)
	U_{eq}	0.0356	0.0335(10)	0.0301(11)	0.0300(14)	0.1075(88)	0.1274(55)	0.187(22)
	occ	1.0	1.0	1.0	1.0	1.0	1.0	1.0
Sr	x	0.2501(1)	0.2579(1)	0.2611(1)	0.2811(3)	0.2801(10)	0.2744(5)	
	y	0.25	0.25	0.25	0.25	0.25	0.25	
	z	0.1780(1)	0.1800(1)	0.1791(1)	0.1838(2)	0.1819(7)	0.1781(3)	
	U_{eq}	0.0151	0.0248(1)	0.0258(2)	0.0556(6)	0.0541(17)	0.0608(8)	
	occ	1.064	1.127(3)	1.207(4)	0.809(5)	0.422(6)	0.350(3)	

Table 2 (*continued*)

		BRNAT	BR24h	BR96h	BR100	BR180	BR330f	BR330s
W1	*x*	0.0598(12)	0.0677(11)	0.0595(18)	0.0849(43)			
	y	0.25	0.25	0.25	0.25			
	z	0.4699(9)	0.4678(10)	0.4674(16)	0.4825(37)			
	U	0.0524	0.0584(17)	0.0682(29)	0.0752(68)			
	occ	1.0	0.876(14)	0.778(20)	0.464(27)			
Sr2	*x*					0.0608(28)	0.0583(12)	0.059(3)
	y					0.25	0.25	0.25
	z					0.5936(24)	0.6059(19)	0.587(4)
	U					0.0770(51)	0.0431(17)	0.078(8)
	occ					0.161(6)	0.106(4)	0.148(8)
W2	*x*	0.9286(9)	0.9362(9)	0.9329(15)	0.9021(34)	0.9103(88)		
	y	0.1474(4)	0.1492(4)	0.1467(7)	0.1476(15)	0.1541(40)		
	z	0.1518(8)	0.1619(8)	0.1623(13)	0.1822(30)	0.1885(72)		
	U	0.0710	0.0802(17)	0.0922(28)	0.0510(52)	0.1452(203)		
	occ	1.0	0.951(12)	0.813(16)	0.280(16)	0.365(29)		
Sr3	*x*						0.8651(68)	0.835(4)
	y						0.1561(31)	0.139(2)
	z						0.1192(62)	0.097(5)
	U						0.1703(146)	0.235(31)
	occ						0.050(4)	0.141(3)
W3	*x*	0.5996(11)	0.5968(9)	0.5892(11)				
	y	0.25	0.25	0.25				
	z	0.0241(11)	0.0214(8)	0.0203(9)				
	U	0.0555	0.0541(14)	0.0474(15)				
	occ	1.0	1.0	1.0				
Sr1	*x*				0.5653(3)	0.5630(8)	0.5618(5)	0.588(3)
	y				0.25	0.25	0.25	0.25
	z				0.0458(3)	0.0585(9)	0.0606(5)	0.060(2)
	U_{eq}				0.396(6)	0.0735(18)	0.0909(10)	0156(9)
	occ				0.484(4)	0.502(6)	0.471(4)	0.282(6)
W4	*x*	0.0665(13)	0.0633(10)	0.0573(14)	0.0479(32)	0.0108(85)	0.9857(48)	
	y	0.25	0.25	0.25	0.25	0.25	0.25	
	z	0.8660(9)	0.8742(9)	0.8685(12)	0.9065(27)	0.9101(69)	0.9031(44)	
	U	0.0539	0.0611(16)	0.0665(23)	0.0651(51)	0.0782(169)	0.1179(98)	
	occ	1.0	0.999(14)	0.961(20)	0.536(26)	0.334(34)	0.394(25)	
Sr4	*x*						0.0631(21)	0.114(8)
	y						0.25	0.25
	z						0.5378(27)	0.438(10)
	U						0.0566(40)	0.214(29)
	occ						0.068(7)	0.122(8)
Sr5	*x*							0.778(7)
	y							0.25
	z							0.929(8)
	U							0.170(22)
	occ							0.098(6)
Sr6	*x*						0.0505(27)	
	y						0.25	
	z						0.6837(33)	

(*continued on next page*)

Table 2 (*continued*)

	BRNAT	BR24h	BR96h	BR100	BR180	BR330f	BR330s
U						0.0357(39)	
occ						0.037(3)	

[a] The correspondence between our labels and those of Ståhl and Hanson [10] is Sr ↔ Sr1, Sr1 ↔ Sr2, Sr2 ↔ Sr3 and Sr3 ↔ Sr4. The nomenclature for water molecule sites is the same as that of Ståhl and Hanson [10].

below [3]) doubled, thus indicating a migration of (Sr,Ba) cations to this site. The occupancy of the other water sites noticeably decreased, leading to a total water molecule number of 3.12. This number could be slightly underestimated if we assume that some water remained in the Sr1 site.

In BR180, the spreading of (Sr,Ba) cations continued, with a further decrease of Sr site occupancy and migration of extra-framework cations to the W1 site (labeled Sr2 below). The water content in the W4 site decreased, leading to a total of 2.12 water molecules and a cell volume reduction of 5% with respect to the original sample.

In both BR100 and BR180, the water loss and volume contraction were accompanied by a contraction of the channels running along the [1 0 0] and [0 0 1] directions.

Samples BR330f and BR330s were heated at the same temperature but for different treatment times: 0.5 and 24 h, respectively. The heating time clearly influenced the degree of dehydration; in fact, only BR330s was completely dehydrated, whereas in BR330f, about one water molecule remained in the channels. Also, the unit cell volume decreased with the heating time, reaching a contraction of 12% in BR330s. It should be noted that the cell volume of BR330f was almost equal to that of BR180 notwithstanding the much higher degree of dehydration, suggesting that the fast heating treatment prevented a collapse of the channels.

In BR330f, the original Sr site further depopulated, and in addition to the Sr1 and Sr2 sites, three other cation sites appeared: Sr3, corresponding to the W2 site, and Sr4 and Sr6, with very low occupancies, which did not correspond to any previous water sites.

In BR330s, the original Sr site was completely empty, Sr1 depopulated, Sr6 was empty, the occupancy of Sr3 increased and a new cation site, Sr5, appeared. Probably, the real spreading of the extra-framework cations was wider than that reported since the number of electrons found in the refinement was lower than that found by chemical analysis.

As regards the framework atoms, the breaking of the T1–O7–T2 bridge began to be observed in BR330f. In this sample, a small quantity (<10%) of tetrahedral cations migrated to the new T11 and T21 sites even if the O71, O72 and O73 oxygens observed in BR280 and in BR330s [3] were not found here (Tables 2 and 3).

In BR330s, the bridge-breaking percentage and migration of tetrahedral cations toward T11 and T21 (in 40% and 24% of cases, respectively) were higher. O71 was completely occupied, while O72 and O73 had an occupancy of 55% and 24%, respectively, higher than in BR280 [3].

4. Discussion

Because the experimental conditions of this work were very different from those of the in situ powder diffraction study [10], the temperature value cannot be used as a comparison parameter. On the contrary, the two studies can be compared on the basis of the unit cell volumes. In the light of this, the refinements made by Ståhl and Hanson [10] at 385, 463, 541 and 621 K can be compared with our refinements of BR24h, BR96h, BR100 and BR180, respectively.

4.1. Water molecules

In Table 1, we observe that the dehydration degree strongly influences the unit cell volume; in particular, the largest variation is on the b parameter and the smallest on the β angle.

Dehydration starts from the W1 and W2 sites, which regularly depopulate during the first stages

Table 3
Bond distances (Å) and selected angles (°) for framework atoms; 8-ring dimension of channels are calculated assuming an oxygen radius of 1.35 Å

	BRNAT	BR24h	BR96h	BR100	BR180	BR330f	BR330s
T1–O1	1.652	1.647(3)	1.648(3)	1.655(4)	1.647(9)	1.640(4)	1.40(3)
T1–O4	1.634	1.631(3)	1.637(3)	1.638(4)	1.624(11)	1.611(5)	1.62(3)
T1–O5	1.651	1.640(3)	1.645(3)	1.639(5)	1.627(8)	1.635(5)	1.66(3)
T1–O7	1.642	1.638(3)	1.636(3)	1.627(5)	1.618(11)	1.623(5)	1.52(3)
Mean	1.645	1.639	1.641	1.640	1.629	1.627	1.55
T11–O1						1.683(29)	1.57(3)
T11–O4						1.669(27)	1.85(3)
T11–O5						1.669(30)	1.69(3)
T11–O71							1.79(3)
Mean						1.674	1.72
T1–T11						1.33(3)	1.35(3)
T2–O1	1.677	1.667(3)	1.664(3)	1.678(5)	1.673(10)	1.696(4)	1.54(3)
T2–O2	1.657	1.658(3)	1.646(4)	1.651(5)	1.618(13)	1.639(6)	1.59(3)
T2–O6	1.656	1.653(3)	1.646(4)	1.635(5)	1.643(12)	1.615(6)	1.55(3)
T2–O7	1.664	1.651(3)	1.645(3)	1.655(5)	1.649(10)	1.643(5)	1.73(3)
Mean	1.664	1.657	1.650	1.655	1.646	1.648	1.60
T21–O1						1.814(43)	1.64(5)
T21–O2						1.657(44)	1.94(4)
T21–O6						1.902(51)	1.81(5)
T21–O72							1.92(4)
T21–O73							2.02(8)
Mean						1.791	1.87
T2–T21						1.53(5)	1.58(4)
T3–O2	1.671	1.657(3)	1.661(3)	1.653(5)	1.645(10)	1.625(5)	1.64(3)
T3–O3	1.671	1.660(3)	1.671(3)	1.661(4)	1.640(10)	1.633(5)	1.62(2)
T3–O4	1.656	1.649(3)	1.651(3)	1.653(4)	1.625(9)	1.631(4)	1.57(3)
T3–O9	1.640	1.638(1)	1.640(2)	1.654(2)	1.608(5)	1.614(3)	1.55(1)
Mean	1.660	1.651	1.656	1.655	1.629	1.625	1.59
T4–O3	1.620	1.616(3)	1.606(3)	1.608(5)	1.565(11)	1.592(5)	1.54(2)
T4–O5	1.614	1.609(3)	1.604(3)	1.618(4)	1.607(9)	1.597(5)	1.54(3)
T4–O6	1.598	1.594(3)	1.600(4)	1.612(5)	1.582(12)	1.592(6)	1.58(2)
T4–O8	1.597	1.590(1)	1.592(1)	1.590(1)	1.561(4)	1.564(1)	1.54(1)
Mean	1.607	1.602	1.600	1.607	1.579	1.586	1.55
T1–O1–T2	133.0	132.8(2)	132.8(2)	130.5(3)	128.3(7)	127.5(3)	135(2)
T2–O2–T3	145.4	145.7(2)	146.8(2)	147.8(3)	148.4(9)	147.8(4)	152(2)
T3–O3–T4	140.1	140.5(2)	140.0(2)	142.0(3)	152.0(9)	151.0(5)	151(1)
T1–O4–T3	146.7	145.2(2)	143.6(2)	137.7(3)	141.7(8)	143.0(4)	149(2)
T1–O5–T4	141.1	141.7(2)	141.8(2)	141.5(3)	142.0(8)	141.1(4)	145(2)
T2–O6–T4	151.9	150.9(2)	150.0(3)	145.6(3)	145.3(8)	147.5(5)	152(2)
T1–O7–T2	136.7	137.9(2)	138.1(2)	140.2(3)	146.8(7)	147.1(3)	152(2)
T4–O8–T4	180.	180.	180.	180.	180.	180.	180.
T3–O9–T3	159.2	157.2(3)	155.5(4)	145.9(4)	149.3(11)	148.1(6)	142(2)
8-ring dimensions along [1 0 0]	2.364 × 5.059	2.313 × 5.022	2.319 × 5.005	2.148 × 4.945	1.868 × 4.945	1.828 × 4.957	1.83 × 4.78
8-ring dimensions along [0 0 1]	2.853 × 4.093	2.794 × 4.076	2.769 × 4.080	2.582 × 4.104	2.698 × 4.085	2.702 × 4.085	2.74 × 3.93

Table 4
Coordination polyhedra of Sr atoms

	BRNAT	BR24h	BR96h	BR100	BR180	BR330f	BR330s
Sr–O1 (2×)	2.889	2.855(3)	2.844(3)	2.743(4)	2.645(10)	2.645(5)	
Sr–O2 (2×)	2.831	2.805(3)	2.833(4)	2.835(6)	2.674(15)	2.643(7)	
Sr–O9	3.183	3.101(5)	3.042(6)	2.827(8)	3.042(28)		
Sr–W1	2.695	2.655(7)	2.700(12)	2.736(28)			
Sr–W2 (2×)	2.827	2.797(6)	2.859(11)	3.126(24)	2.996(63)		
Sr–W3	2.740	2.685(6)	2.623(7)				
Sr–W4	2.634	2.614(7)	2.666(9)	2.544(21)	2.654(55)	2.757(34)	
Sr1–O1 (2×)				2.812(5)	2.669(10)	2.643(5)	2.80(3)
Sr1–O2 (2×)					3.309(17)	3.174(9)	2.90(3)
Sr1–O4 (2×)				3.038(5)	3.224(13)	3.280(7)	3.30(3)
Sr1–O72							2.83(5)
Sr1–O73 (2×)							3.25(7)
Sr1–O9				3.263(7)	3.291(23)		
Sr1–W2 (2×)				3.014(24)	2.970(62)		
Sr1–W4				3.532(7)	3.328(26)	3.208(7)	
Sr2–O3 (2×)					3.015(18)	3.019(9)	2.84(2)
Sr2–O4 (2×)					3.111(19)	3.085(9)	3.02(3)
Sr2–O5 (2×)					3.012(16)	2.970(9)	3.07(3)
Sr2–O72							3.12(6)
Sr2–O73 (2×)							2.39(8)
Sr2–O9					3.210(32)	3.041(17)	2.83(4)
Sr2–W4					2.470(56)	2.367(36)	
Sr3–O2							3.00(4)
Sr3–O5							3.10(4)
Sr3–O6							3.21(4)
Sr3–O7						3.272(50)	2.91(4)
Sr3–O72							3.08(5)
Sr3–O73							3.22(7)
Sr3–W4						2.482(55)	
Sr4–O2 (2×)							3.25(5)
Sr4–O3 (2×)						3.054(12)	
Sr4–O4 (2×)						3.194(14)	3.20(6)
Sr4–O5						3.220(13)	
Sr4–O71							2.49(8)
Sr4–O9						3.029(21)	3.24(6)
Sr4–W4						2.887(38)	
Sr5–O4 (2×)							3.25(5)
Sr5–O71							2.52(6)
Sr5–O73 (2×)							3.12(9)
Sr5–O9							3.25(7)
Sr6–O3 (2×)						3.079(15)	
Sr6–O4 (2×)						3.080(16)	
Sr6–O5 (2×)						2.782(9)	
Sr6–O9						3.148(25)	

and then, in BR180 and BR330f, are partially occupied by (Sr,Ba) cations. The W3 site is fully occupied by water molecules up to BR96h, and substituted by cations in BR100. W4 is the last site involved in the dehydration process; its occupancy halves in BR100 and falls to zero only in BR330s.

These results are in agreement with the dehydration mechanism reported by Ståhl and Hanson [10], assuming that their highest temperature sample corresponds to our BR180. On the contrary, the following structural features, reported by Ståhl and Hanson [10], were not observed in this work:

- the appearance of the W12 site at 420 K and its disappearance at 620 K;
- the presence of the new water site W11 above 541 K;
- the presence of all the water sites up to 621 K even if with low occupancies.

4.2. Extra-framework cation sites

During the dehydration process, a depopulation of the original Sr site and a spreading of extra-framework cations to sites previously occupied by water molecules is observed (Fig. 2). The Sr coordination polyhedron shows a decrease of the coordination number and of the bond distances from the framework oxygens. The new cation sites show very irregular coordination polyhedra, with very long distances from both the framework and the water molecule oxygens. In these polyhedra, only two framework oxygens and/or one water molecule are at acceptable coordination distances.

The two samples dehydrated at 330°C for different times show a different distribution of extra-framework cations, indicating that cation spreading is dependent also on the heating time.

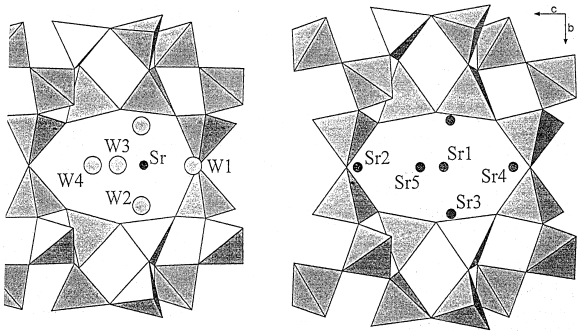

Fig. 2. 8-ring channel parallel to [1 0 0] in BR24h (left) and in BR330s (right). T11 and T21 polyhedra are omitted in the drawing for the sake of clarity. The non-labeled Sr atom is related to Sr3 by a mirror plane.

A possible rationalization of the spreading of cations could be based on the bond strength of the framework oxygens, as already reported for the dehydration processes of amicite [14] and scolecite [15]. In fact, in BRNAT, all the framework oxygens are coordinated to tetrahedral sites, statistically occupied by silicon or aluminum, with the exception of O8, which is coordinated to two T4 sites occupied by silicon alone. Consequently, their charge balance will be obtained via the contribution of the extra-framework species. In particular, O1, O2 and O9 are involved in bonds with the Sr site, whereas the other oxygens, with the exception only of O6, generally have weak hydrogen bonds with all the water molecules. Starting from BR100, the water content of which is drastically lower than that of BRNAT, the cations in the Sr site approach O1, O2 and O9, and spreading over new sites begins to be observed. In this way, each oxygen, which has lost its bonded water molecules, is now coordinated to at least two cation sites. The same charge balance effect could not have been obtained by the localization of the cations in a single site.

4.3. Framework

During the dehydration process, the tetrahedra maintain a regular shape, with a minor decrease of the mean T–O values. The (Si,Al) distribution is disordered in T1, T2 and T3, whereas only Si is present in T4, as observed in the untreated brewsterite (BRNAT).

The 8-ring channel parallel to [1 0 0] shows a strong contraction in the *b* direction, whereas that parallel to [0 0 1] shows a less pronounced contraction, but always in the *b* direction. The modifications of the T–O–T angles associated with this collapse of the channels are deducible from Table 3 and Fig. 2. In particular, we can observe a large reduction of the T3–O9–T3 angle, accompanied by a compensatory increase of the T3–O3–T4 angle with a rotation of the T3 tetrahedron. Consequently, there is also a large increase of the T1–O7–T2 angle (Table 3). The angle variations reported in this study are, however, considerably

smaller than those reported by Ståhl and Hanson [10], thus suggesting a more flexible behavior of brewsterite when exposed to the experimental conditions applied in the in situ experiment with respect to those used in this work.

Only when dehydration is almost complete is the T1–O7–T2 breaking observed, i.e., in BR330f and BR330s. This could be the response of the structure to the strain induced on the framework oxygens by collapse of the channels, and by the new coordination demand of the exchangeable cations. The fact that the breaking occurs on a bridge of the 4-membered ring is not surprising since this behavior is common to all interrupted frameworks of the dehydrated zeolites of the heulandite group.

As observed by Alberti et al. [3], the higher the heating temperature, the higher the percentage of bridge breaking. In this work, we demonstrate that the treatment time also influences the breaking degree. In fact, the BR330f sample, heated for only 30 min, shows a lower breaking percentage with respect to both the brewsterite heated at 280°C for 24 h and the sample heated at 330°C for 24 h.

The feature common to all the dehydrated brewsterites with interrupted framework (BR280 [3], BR330f and BR330s (this work) is the nearly complete absence of water molecules in the channels. Therefore, this situation seems to be essential for T–O–T bridge breaking. This conclusion is also consistent with the results of the in situ powder diffraction experiments, where the existence of residual water molecules prevents framework interruption.

Acknowledgements

The authors are indebted to Prof. Alberto Alberti for the thorough and constructive suggestions and to Luca Pelosi for his assistance in the dehydration experiments. Italian CNR and MURST (“Transformations, reactions, ordering in minerals” COFIN 1999) are acknowledged for the financial support.

References

[1] J.L. Schlenker, J.J. Pluth, J.V. Smith, Acta Crystallogr. B33 (1977) 2907.
[2] A. Artioli, J.V. Smith, Å. Kvick, Acta Crystallogr. 41 (1985) 492.
[3] A. Alberti, M. Sacerdoti, S. Quartieri, G. Vezzalini, Phys. Chem. Miner. 26 (1999) 181.
[4] A. Alberti, G. Vezzalini, in: L.B. Sand, F.A. Mumpton (Eds.), Natural Zeolites. Occurrence, Properties, Use, Pergamon Press, Oxford, 1978, p. 85.
[5] A. Alberti, R. Rinaldi, G. Vezzalini, Phys. Chem. Miner. 2 (1978) 365.
[6] A. Alberti, G. Vezzalini, TMPM Tschermaks Min. Petr. Mitt. 31 (1983) 259.
[7] A. Alberti, G. Vezzalini, in: D. Olson, A. Bisio (Eds.), Proceedings of the Sixth International Zeolite Conference Reno, Butterworth, Guildford, UK, 1984, p. 834.
[8] G. Cruciani, G. Artioli, A. Gualtieri, K.C. Ståhl, J.C. Hanson, Am. Mineral. 82 (1997) 729.
[9] A. Alberti, G. Vezzalini, S. Quartieri, G. Cruciani, S. Bordiga, Micropor. Mesopor. Mater., submitted for publication.
[10] K. Ståhl, J.C. Hanson, Micropor. Mesopor. Mater. 32 (1999) 147.
[11] G.M. Sheldrick, A program for crystal structure determinations, University of Goettingen, Germany, 1993.
[12] T. Armbruster, T. Kohler, N. Jb. Miner Mh. 1992 (1992) 385.
[13] G. Vezzalini, S. Quartieri, A. Alberti, Zeolites 13 (1993) 34.
[14] G. Vezzalini, A. Alberti, A. Sani, M. Triscari, Micropor. Mesopor. Mater. 31 (1999) 253.
[15] K. Ståhl, J.C. Hanson, J. Appl. Crystallogr. 27 (1994) 543.
[16] A.C. North, D.C. Phillips, F.S. Mathews, Acta Crystallogr. A24 (1968) 351.
[17] R.H. Blessing, J. Appl. Cryst. 30 (1997) 421.
[18] N. Walker, D. Stuart, Acta Crystallogr. A39 (1983) 158.